Transaction of the Korean Society of Mechanical Engineers, Vol. 9, No. 1, pp. 109~118, 1985.

<Original>

The Computation of Stress Intensity Factors in Fiberreinforced Composites using a Contour Integral Method

Jin Woo Kim* and Heung Suk Chang**

(Received July 20, 1984)

경로적분법에 의한 섬유강화복합재의 응력확대계수 계산

김 진 우·장 흥 석

초 록

특이응력해석을 위한 일반화된 가역상반일 경계적분식이 섬유강화복합재를 모형화한 직교 이방성 크랙평판의 수치해를 위하여 발전시켰다. 이 적분방정식은 평판경계에서의 탄성변위와 트랙션의 변수로 구성된 경계적분식의 형태로 하중이 없다는 두 크랙면의 경계조건과 유한의 탄성변형에너지의 개념에서 경계적분식에 필요한 특성해를 규정하고 대응되는 보조해를 계산하였다. 직교이방도를 달리한 중앙크랙평판의 응력확대계수를 계산하여 기존해와 비교하였다. 또한 대칭모우드 I 형의 양측 크랙평판 및 복합모우드형 편측크랙 일단고정 평판의 응력확대계수가 임의의 섬유방향각에 따라서 계산되었다.

1. Introduction

The crack tip singularity in rectilinearly anisotropic materials, as observed by Sih et al.[1] can be completely characterized in the same manner as in the isotropic case by properly defining anisotropic stress intensity factors (SIF). Determination of the SIF is thus an important design aspect for assessing fracture strength of the anisotropic composite structural components. Within the framework of plane, linear elastic fracture mechanics, a problem of continuing interest is the calculation of the SIF in the cracked orthotropic plates modelling the fiber-reinforced composites. Many different numerical methods developed for isotropic materials have been extended to treat some problems involving anisotropic materials including the mapping-collocation method of Bowie and Freeze[2], the displacement hybrid element of Atluri et.al.[3], and a conservation integral method introduced recently by Wang, Yau and Corten[4,5,6]. Among these a contour

*Member, Dept. of Mechanical Engineering, Korea Military Academy

**Graduate student, Dept. of Mechanical Engineering, Chung-Ang University

integral method proposed by Stern[7] is attractive one due to its numerical simplicity and computational efficiency. This method is based on the Betti's reciprocal work theorem from which the singular stress intensities at the crack tip can be evaluated in terms of an path independent integral involving the tractions and displacements on a contour boundary remote from the crack tip. Thus this method is easily incorporated into most exsiting finite element stress analysis programs which have no provision for treating singular stress states. The terms representing the singular intensities can be obtained explicitly by a routine evaluation of the reciprocal work of the product functions between the characteristic singular solutions and corresponding complementary elastic states defined on the neighborhood of the singular point. With identification of such singular functions there have been successful applications of the method to the various types of singularity problems in isotropic materials[8,9] as well as in dissimilar media[10]. For the orthotropic composite materials Soni and Stern[11] also developed the desired characteristic singular functions by using two complex potentials in anisotropic elasticity theory of Green and Zerna[12], and England's singularity representation[13]. Demonstration of the extension, however, were still restricted to illustrate the general orthotropic singular behavior in view of dealing orthotropic configurations where the crack axis is always parallel to one of the principal directions of material symmetry corresponding to the fiber direction.

The purpose of present work is to extend the contour integral method to treat the general orthotropic plates with crack. While the basic method follows closely in spirit the ideas outlined in[7] the formulation of the problem is different in the use of new characteristic singular solutions. In the next section the contour integral representation is outlined and the singular solutions required can be identified. The corresponding complementary elastic states are constructed on the basis of the traction free boundary conditions of crack edge and the concept of finite reciprocal work on the contour enclosing the crack tip. The computational procedures newly adopted for the SIF are described in section 3. Finally the results of numerical computation for some typical orthotropic elastic plates are presented in section 4.

2. Contour Integral Formulation

The integral representation outlined in[7] can be started from the Betti's reciprocal work theorem for plane elastic states with vanishing body forces;

$$\int_{\partial R^*}(\underset{\sim}{T}\cdot\underset{\sim}{u}^c-\underset{\sim}{T}^c\cdot\underset{\sim}{u})\mathrm{ds}=0 \qquad (1)$$

Here $\underset{\sim}{u}$ is the displacement field and $\underset{\sim}{T}$ the traction vector on the boundary ∂R^* of a simply connected and bounded region R^*, corresponding to the solution of any particular equilibrium problem; $\underset{\sim}{u}^c$ and $\underset{\sim}{T}^c$ are the displacement and traction corresponding to any other such problem.

In order to apply the reciprocal work theorem to a body with an edge crack we first delete from the body points within a circle of radius ε centered at the crack tip as indicated in Fig. 1.

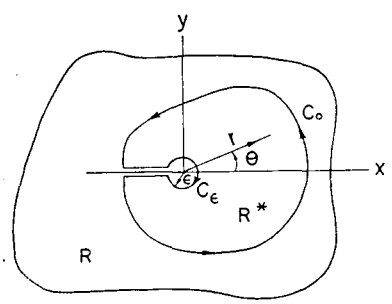

Fig. 1 Deleted region for a singularity

The boundary of the remaining body is decomposed into two parts; the circular boundary of the deleted region, denoted C_ε, and the remaining boundary denoted C_0. Then Eq. (1) becomes

$$I_\varepsilon = -\int_{C\varepsilon}(\underset{\sim}{T}\cdot\underset{\sim}{u}^c - \underset{\sim}{T}^c\cdot\underset{\sim}{u})\,ds = \int_{C_0}(\underset{\sim}{T}\cdot\underset{\sim}{u}^c - \underset{\sim}{T}^c\cdot\underset{\sim}{u})\,ds \tag{2}$$

and the idea now is to evaluate these integrals for arbitrarily small ε and suitable choice of the complementary equilibrium state.

We suppose that for the equilibrium stress state of interest, the crack faces are free of traction and on the remainder of the boundary either the displacement or the traction components in the normal and tangential directions are prescribed so that we have a well posed problem. The stresses and displacements in the neighbornood of the crack tip in rectilinearly anisotropic media are then known to have the following forms[14]

$$\begin{aligned}
u_x^s &= \sqrt{\frac{2r}{\pi}}\,\mathrm{Re}\Big\{\frac{1}{\gamma_2-\gamma_1}[(\gamma_2 p_1\sqrt{\cos\theta-\gamma_1\sin\theta} - \gamma_1 p_2\sqrt{\cos\theta-\gamma_2\sin\theta})K_{\mathrm{I}} \\
&\quad + (p_2\sqrt{\cos\theta-\gamma_2\sin\theta} - p_1\sqrt{\cos\theta-\gamma_1\sin\theta})\theta K_{\mathrm{II}}]\Big\} \\
u_y^s &= \sqrt{\frac{2r}{\pi}}\,\mathrm{Re}\Big\{\frac{1}{\gamma_2-\gamma_1}[(\gamma_2 q_1\sqrt{\cos\theta-\gamma_1\sin\theta} - \gamma_1 q_2\sqrt{\cos\theta-\gamma_2\sin\theta})K_{\mathrm{I}} \\
&\quad + (q_2\sqrt{\cos-\gamma_2\sin\theta} - q_1\sqrt{\cos\theta-\gamma_1\sin\theta})K_{\mathrm{II}}]\Big\} \\
\sigma_x^s &= \frac{K_{\mathrm{I}}}{\sqrt{2\pi r}}\,\mathrm{Re}\Big[\frac{\gamma_1\gamma_2}{\gamma_2-\gamma_1}\Big(\frac{\gamma_1}{\sqrt{\cos\theta-\gamma_1\sin\theta}} - \frac{\gamma_2}{\sqrt{\cos\theta-\gamma_2\sin\theta}}\Big)\Big] \\
&\quad + \frac{K_{\mathrm{II}}}{\sqrt{2\pi r}}\,\mathrm{Re}\Big[\frac{1}{\gamma_2-\gamma_1}\Big(\frac{\gamma_2^2}{\sqrt{\cos\theta-\gamma_2\sin\theta}} - \frac{\gamma_1^2}{\sqrt{\cos\theta-\gamma_1\sin\theta}}\Big)\Big] \\
\sigma_y^s &= \frac{K_{\mathrm{I}}}{\sqrt{2\pi r}}\,\mathrm{Re}\Big[\frac{1}{\gamma_2-\gamma_1}\Big(\frac{\gamma_2}{\sqrt{\cos\theta-\gamma_1\sin\theta}} - \frac{\gamma_1}{\sqrt{\cos\theta-\gamma_2\sin\theta}}\Big)\Big] \\
&\quad + \frac{K_{\mathrm{II}}}{\sqrt{2\pi r}}\,\mathrm{Re}\Big[\frac{1}{\gamma_2-\gamma_1}\Big(\frac{1}{\sqrt{\cos\theta-\gamma_2\sin\theta}} - \frac{1}{\sqrt{\cos\theta-\gamma_1\sin\theta}}\Big)\Big] \\
\tau_{xy}^s &= \frac{K_{\mathrm{I}}}{\sqrt{2\pi r}}\,\mathrm{Re}\Big[\frac{\gamma_1\gamma_2}{\gamma_2-\gamma_1}\Big(\frac{1}{\sqrt{\cos\theta-\gamma_1\sin\theta}} - \frac{1}{\sqrt{\cos\theta-\gamma_2\sin\theta}}\Big)\Big] \\
&\quad + \frac{K_{\mathrm{II}}}{\sqrt{2\pi r}}\,\mathrm{Re}\Big[\frac{1}{\gamma_2-\gamma_1}\Big(\frac{\gamma_2}{\sqrt{\cos\theta-\gamma_2\sin\theta}} - \frac{\gamma_1}{\sqrt{\cos\theta-\gamma_1\sin\theta}}\Big)\Big]
\end{aligned} \tag{3}$$

where γ_1, γ_2 are the roots of the following characteristic equation

$$C_{11}\gamma^4 - 2C_{16}\gamma^3 + (2C_{12}+C_{66})\gamma^2 - 2C_{26}\gamma + C_{22} = 0 \tag{4}$$

C_{ij}, $i,j=1,2,6$ are symmetric elastic compliance coefficients. Note that the roots of Eq. (4) are always complex or purely imaginary and occur in conjugate pairs as γ_1, $\bar{\gamma}_1$ and γ_2, $\bar{\gamma}_2$

Here also $p_k = C_{11}\gamma_k^2 + C_{12} + C_{16}\gamma_k$

$$q_k = -C_{12}\gamma_k - C_{22}/\gamma_k - C_{26},\quad k=1,2 \tag{5}$$

The anisotropic stress intensity factor can be introduced as

$$\begin{aligned}
K_{\mathrm{I}} &= \lim_{r\to 0}\sqrt{2\pi z}\;\sigma_y|_{\theta=0} \\
K_{\mathrm{II}} &= \lim_{r\to 0}\sqrt{2\pi z}\;\tau_{xy}|_{\theta=0}
\end{aligned} \tag{6}$$

where $z = r\,e^{i\theta}$ complex variable.

The complementary elastic state to be used in the reciprocal work relation can be derived in the Appendix and has the form

$$\begin{aligned}
u_x^c &= \frac{2}{\sqrt{r}}\,\mathrm{Re}\Big\{\frac{1}{\gamma_2-\gamma_1}\Big[\Big(\frac{\gamma_1 p_2}{\sqrt{\cos\theta-\gamma_2\sin\theta}} - \frac{\gamma_2 p_1}{\sqrt{\cos\theta-\gamma_1\sin\theta}}\Big)C_1 \\
&\quad + \Big(\frac{p_1}{\sqrt{\cos\theta-\gamma_1\sin\theta}} - \frac{p_2}{\sqrt{\cos\theta-\gamma_2\sin\theta}}\Big)C_2\Big]\Big\} \\
u_y^c &= \frac{2}{\sqrt{r}}\,\mathrm{Re}\Big\{\frac{1}{\gamma_2-\gamma_1}\Big[\Big(\frac{\gamma_1 q_2}{\sqrt{\cos\theta-\gamma_2\sin\theta}}
\end{aligned}$$

$$-\frac{\gamma_2 q_1}{\sqrt{\cos\theta-\gamma_1\sin\theta}}\Big)C_1$$
$$+\Big(\frac{q_1}{\sqrt{\cos\theta-\gamma_1\sin\theta}}$$
$$-\frac{q_2}{\sqrt{\cos\theta-\gamma_2\sin\theta}}\Big)C_2\Big]\Big\}$$

$$\sigma_x{}^c=\frac{1}{r^{3/2}}\mathrm{Re}\Big\{\frac{1}{\gamma_2-\gamma_1}\Big[\gamma_1\gamma_2\Big(\frac{\gamma_1}{(\cos\theta-\gamma_1\sin\theta)^{3/2}}$$
$$-\frac{\gamma_2}{(\cos\theta-\gamma_2\sin\theta)^{3/2}}\Big)C_1$$
$$+\Big(\frac{\gamma_2{}^2}{(\cos\theta-\gamma_2\sin\theta)^{3/2}}$$
$$-\frac{\gamma_1{}^2}{(\cos\theta-\gamma_1\sin\theta)^{3/2}}\Big)C_2\Big]\Big\} \tag{7}$$

$$\sigma_y{}^c=\frac{1}{r^{3/2}}\mathrm{Re}\Big\{\frac{1}{\gamma_2-\gamma_1}\Big[\Big(\frac{\gamma_2}{(\cos\theta-\gamma_1\sin\theta)^{3/2}}$$
$$-\frac{\gamma_1}{(\cos\theta-\gamma_2\sin\theta)^{3/2}}\Big)C_1$$
$$+\Big(\frac{1}{(\cos\theta-\gamma_2\sin\theta)^{3/2}}$$
$$-\frac{1}{(\cos\theta-\gamma_1\sin\theta)^{3/2}}\Big)C_2\Big]\Big\}$$

$$\tau^c{}_{xy}=\frac{1}{r^{3/2}}\mathrm{Re}\Big\{\frac{1}{\gamma_2-\gamma_1}\Big[\gamma_1\gamma_2\Big(\frac{1}{(\cos\theta-\gamma_1\sin\theta)^{3/2}}$$
$$-\frac{1}{(\cos\theta-\gamma_2\sin\theta)^{4/2}}\Big)C_1$$
$$+\Big(\frac{\gamma_2}{(\cos\theta-\gamma_2\sin\theta)^{3/2}}$$
$$-\frac{\gamma_1}{(\cos\theta-\gamma_1\sin\theta)^{3/2}}\Big)C_2\Big]\Big\}$$

where C_1 and C_2 are arbitrary constants.

Now on the inner circular boundary C_ε the evaluation of the contour integral in terms of the traction and displacement components(writing in polar coordinate system) takes the form

$$I_\varepsilon=-\int_{C\varepsilon}(\underset{\sim}{T}\cdot\underset{\sim}{u}^c-\underset{\sim}{T}^c\cdot\underset{\sim}{u})\mathrm{ds}$$
$$=\int_{-\pi}^{\pi}(\sigma_r{}^c u_r{}^s+\tau^c{}_{r\theta}u_\theta{}^s-\sigma_r{}^s u_r{}^c-\tau^s{}_{r\theta}u_\theta{}^c)r\,d\theta \tag{8}$$

Upon substitution from the forgeing singular solutions (3) and complementary ones (7), a routine evaluation or an appropriate numerical quadrature of the integral produces symbolically

$$I_\varepsilon=(J_1{}^{\mathrm{I}}C_1+J_2{}^{\mathrm{I}}C_2)K_{\mathrm{I}}$$
$$+(J_1{}^{\mathrm{II}}C_1+J_2{}^{\mathrm{I}}C_2)K_{\mathrm{II}} \tag{9}$$

where the quantities $J_i{}^{\mathrm{I}}$, $J_i{}^{\mathrm{II}}$, $i=1,2$ can be computed using Eqs. (3) and (7) once the elastic properties of the material are given.

Consequently, for arbitrarily small ε Eq. (2) yields the representation formula for the SIF

$$(J_1{}^{\mathrm{I}}C_1+J_2{}^{\mathrm{I}}C_2)K_{\mathrm{I}}+(J_1{}^{\mathrm{II}}C_1+J_2{}^{\mathrm{II}}C_2)K_{\mathrm{II}}$$
$$=\int_{C_0}(\underset{\sim}{T}\cdot\underset{\sim}{u}^c-\underset{\sim}{T}^c\cdot\underset{\sim}{u})ds \tag{10}$$

where it is important to note that the contour C_0 involves only the outer boundary since both $\underset{\sim}{T}$ and $\underset{\sim}{T}^c$ necessarily vanish on the crack faces. It remains only to obtain $\underset{\sim}{u}$ and $\underset{\sim}{T}$ on the outer boundary from the prescribed data so that the contour integral may be evaluated as a linear combination of C_1 and C_2, the coefficients of which are the desired stress intensity factors, K_{I} and K_{II}.

3. Computational Procedures

The evaluation of the integral on the right-hand side of (10) involves the complementary functions (7) and the tractions and displacements along the contour C_0. A FEM including 4, 8 node quadrilateral elements in plane stress analysis was used to obtain the traction and displacement data on the boundary C_0. The contour C_0 was chosen to pass through Gaussian quadrature rule integration points in the interior of each element as shown in Fig. 2(a) so that the stress components generated by the FEM solutions can be directly used for an appropriate numerical quadrature on C_0. A linearly (or quadratically for 8 node quadrilateral element) varying displacement furnished from the FEM solutions can be evaluated at the integration points on C_0. Fig. 2(b) depicts a special treatment of a corner element which might be a part of contour. Both traction vectors and displacements at a and b is first determined by interpolating the values at (â, ă) and ($\hat{\mathrm{b}}$, $\check{\mathrm{b}}$) respectively of two adjacent elements. Then

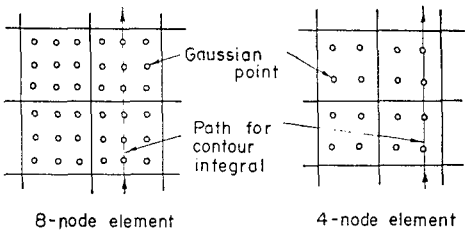

Fig. 2(a) Gaussian points and integration path for a boundary integral

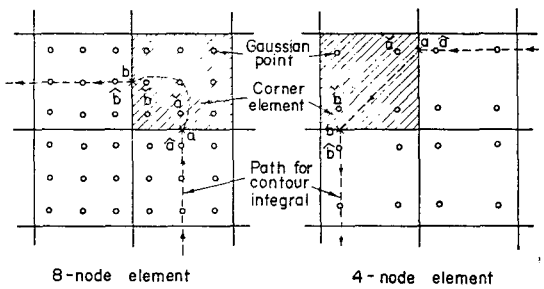

Fig. 2(b) Integration path through the corner element

use these values at a and b for interpolating again the tractions and displacements to be evaluated at the corresponding integration points of the corner element.

With the tractions and displacements furnished by the finite element analysis and the complementary solutions ($\underset{\sim}{T}^c$, $\underset{\sim}{u}^c$) known to be within multiplicative constants C_1 and C_2 from (7), the reciprocal work can be computed for each interior of element forming the contour C_0 and these values accumulated. The resulting quantities thus obtained are deneted by I_1 and I_2. Then we have finally

$$(J_1^{\mathrm{I}}C_1+J_2^{\mathrm{I}}C_2)K_{\mathrm{I}}+(J_1^{\mathrm{II}}C_1+J_2^{\mathrm{II}}C_2)K_{\mathrm{II}} =I_1C_1+I_2C_2 \qquad (11)$$

The two SIF in the equations are then determined by choosing the constants C_1 and C_2 (for example, $C_1=1$ and $C_2=0$ for symmetric mode I case) so that the complementary solutions pick up only the symmetric or skew symmetric components of the actual elastic field.

4. Numerical Results

The procedures as outlined above have been programmed for the general case of plane rectilinear anisotropy. Accuracy of the develdope code was assessed by analyzing a centrally cracked orthotropic tension plate and comparing the obtained results with the boundary collocations by Bowie and Freeze[2] Principal directions of the orthotropic material were alined in the two lines of symmetry and therefore only one quadrant of the plate considered in this analysis. The FEM grid for a quadrant of the plate is shown in Fig. 3 which also depicts the integration contours used for evaluation by dotted lines. The material properties being considered are in terms of ratios of modulus of elasticity E_x/E_y=0.3, 0.5, 0.7, 0.9, 1.5 and 3.5.

The results (evaluated on the path A of exterior contour) plotted in Fig. 4 show the normalized SIF, and indicate very good agreement between present contour integral computation and those in[2] of Bowie and Freeze. As can be seen from Table 1, the calculation is

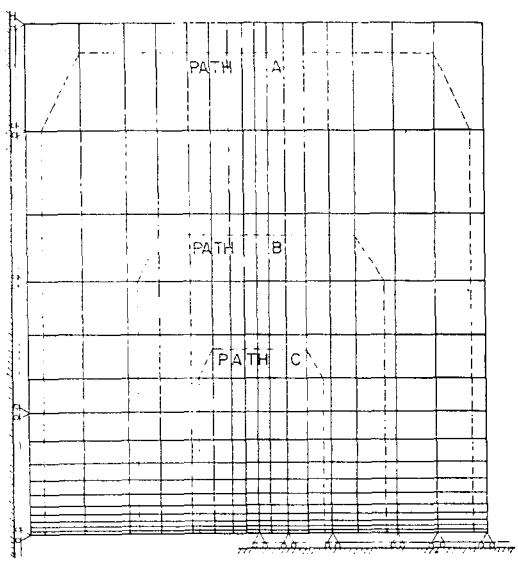

Fig. 3 Finite element grid and integration contour for a quadrant

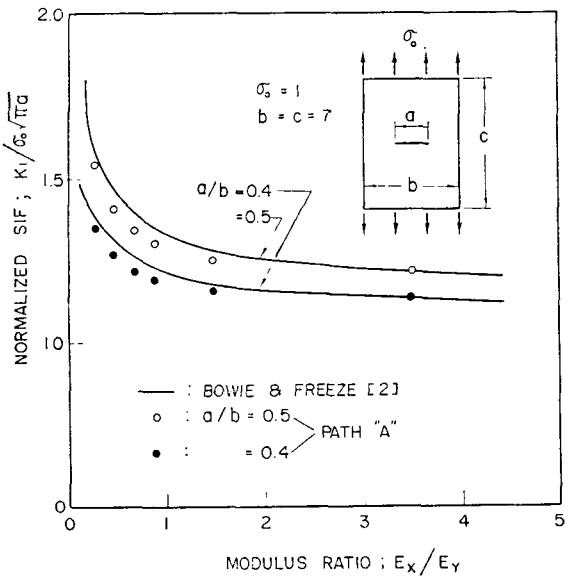

Fig. 4 The normalized SIF in orthotropic tension plate with central crack

Table 1 The normalized SIF in centrally cracked tension plate with various degree of orthotropy

$K_I/\sigma_0\sqrt{\pi a}$	a/b	E_x/E_y part	0.3	0.5	0.7	0.9	1.5	3.5
	0.4	[2]	1.37	1.30	1.26	1.23	1.18	1.13
		Path A	1.343	1.251	1.209	1.182	1.149	1.130
		Path B	1.339	1.246	1.204	1.178	1.146	1.129
		Path C	1.332	1.237	1.195	1.169	1.139	1.123
	0.5	[2]	1.57	1.46	1.39	1.35	1.28	1.22
		Path A	1.539	1.399	1.337	1.296	1.248	1.211
		Path B	1.535	1.394	1.331	1.290	1.244	1.209
		Path C	1.528	1.386	1.322	1.282	1.237	1.203

stable with regard to contour selection and convergent to the choice of outer contour.

For further illustrative numerical examples two cracked orthotropic plates modelling bidirectional fiber-reinforced composites have been treated; symmetric mode I type of double edge crack tension plate and mixed mode type of cantilever plate with a single edge crack. Fig. 5 shows that the bidirectional fiber orientations are arranged at$\pm\alpha$ to the principal material direction 1, where α is the angle between the crack axis and the fiber direction. It should be noted here the elastic compliance coefficients in Eq. (4) can be calculated by the same transformation rule as for the off-axis unidirectional fiber composites[15] except the vanishing terms of C_{16} and C_{26}. Same argument is also applicable to establish the elastic stiffness matrix. This implies, in other word, there appear no coupling terms between normal stresses and shear stresses. The elastic moduli data used in both cases are

$E_{11}=21\times10^6$psi

$E_{22}=1.7\times10^6$psi

$G_{12}=1.4\times10^6$psi

$\nu_{12}=0.21$

which is representive of fiber-reinforced graphite/epoxy composites. Note that subscript 1 indicates the direction parallel to fiber orientation.

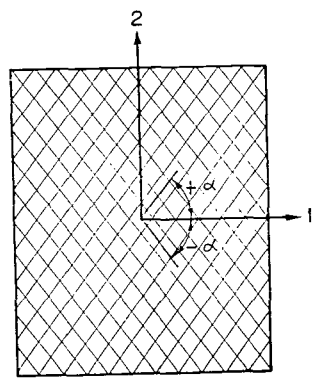

Fig. 5 Symmetry axes in bidirectional fiber-reinforced composite

For the first problem, tthe double edge crack subjected to a uniform tension, the FEM model of a quadrant of the plate is the same as in Fig. 3. The normalized SIF for various fiber angles were computed and tabulated in Table 2. As evaluated on path B Fig. 6 gives the variation of the SIF with fiber orientations. For comparative purposes, the corresponding isotropic solution can be obtained using present

method as well as other approach[16] and plotted also in Fig. 6. Results show that K_I gradually decreses to a minimum as α approaches 40° and then increases with the increase of the fiber angle. The value of K_I at $\alpha=70°$ is approximately equal to the value of isotropic case. The behavior displayed in Fig. 6 may be qualitatively similar trend to that by Mandell et al.[17] who have shown in the symmetric angle-ply composites analysis its minimum at $\alpha=37.5°$ and the value at $\alpha=55°$ equal to that of isotropic case. It can be also seen from Table 2 the calculation is stable with regard to contour selection and there appears the maximum difference of 4.5 percent at $\alpha=40°$ between the values for path A and C.

Table 2 The normalized SIF in bidirectional composite plate with double edge crack

Fiber angle	$K_I/\sigma_0\sqrt{\pi a}$		
	Path A	Path B	Path C
0	1.080	1.077	1.081
10	1.044	1.036	1.037
20	0.984	0.969	0.967
30	0.919	0.900	0.893
40	0.865	0.844	0.828
50	0.890	0.866	0.849
60	1.006	0.992	0.986
70	1.264	1.265	1.270
80	1.855	1.850	1.856
90	2.464	2.443	2.440
*	1.288	1.273	1.276

* Corresponding isotropic solutions where Paris & Sih[16] get the value of 1.274

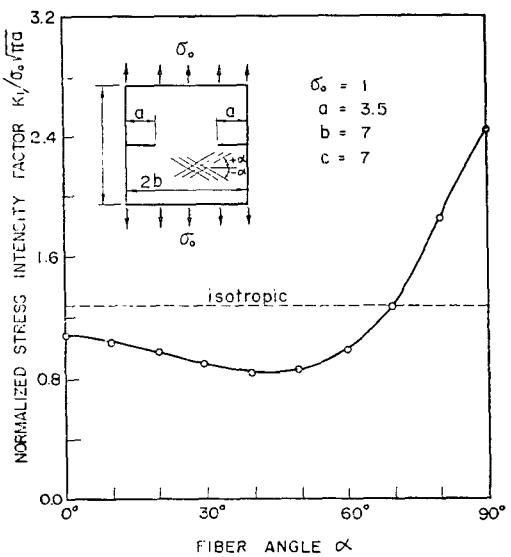

Fig. 6 Effect of fiber angle in double edge cracked tension plate

The second problem, a mixed mode type of cantilever plate subjected to end shear, was analyzed with 240 elements over full length of the plate as shown in Fig. 7. The resulting SIF are plotted in Fig. 8 and listed in Table 3. K_I curve indicates a minimum value at $\alpha=50°$ and the value at $\alpha=80$ approximately reaches to the value of isotropic case. Although the values of K_I differ from the forgeing double edge crack plate, the shape of the curve shows qualitatively same behavior with variation of fiber angle. The effect of fiber angle on the antisymmetric SIF, K_{II} is somewhat different. K_{II} curve moves down monotonically with increase of fiber angle being always smaller values than that for isotropic case. In this mixed mode analysis there appears K_I to be a

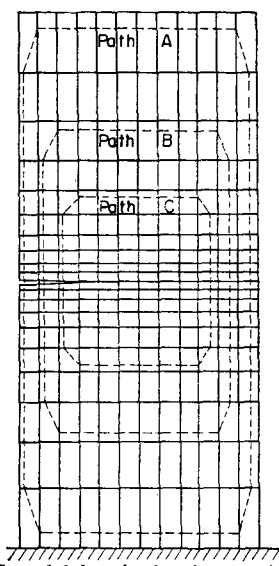

Fig. 7 FEM model for single edge cracked cantilever plate

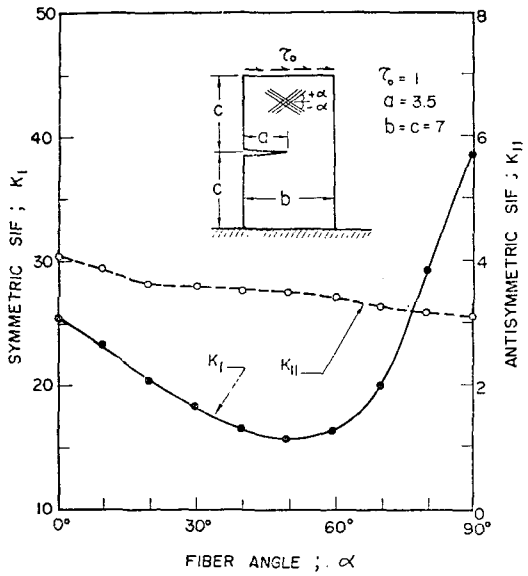

Fig. 8 Effect of fiber angle in single edge cracked cantilever plate

Table 3 The mixed mode K_I and K_{II} in bidirectional composite cantilever plate with single edge crack

Path / SIF / Angle	B		C	
	K_I	K_{II}	K_I	K_{II}
0	25.30	4.082	25.10	4.131
10	23.28	3.875	23.31	3.895
20	20.30	3.619	20.69	3.597
30	18.29	3.600	19.20	3.553
40	16.46	3.545	18.23	3.521
50	15.72	3.485	18.21	3.542
60	16.31	3.403	18.96	3.519
70	19.91	3.238	22.32	3.331
80	29.20	3.114	30.89	3.115
90	38.55	3.098	39.49	3.030
*	28.53	4.512	28.35	4.495

* Corresponding isotropic solutions

significant discrepancy of around maximum 13 percent between the results calculated on path B and C near at the fiber angle $\alpha=50°$ where solutions of forgeing double edge crack problem also show a notable deviation at such a consistent place with different choice of contour. The source of this discrepancy has not yet been identified. However it might be significant to note that for the fiber angle around $\alpha=50°$ the transformed elastic properties of the material could have adverse effects on modelling in the neighborhood of the cracktip. This might be the case that variation of the elastic constants with α exhibits both E_x and E_y smaller values and G_{xy} greater value. This might result in crude solutions of roots of the characteristic polynomial (4), and these solutions then get into formation of the singular solutions as well as complementary ones.

5. Conclusions

An exsiting boundary integral technique for calculating the SIF can be extended to treat the cracked orthotropic elastic plates. The characteristic singular functions governing in the neighborhood of crack tip can be identified and corresponding complementary elastic states are constructed on the basis of traction free boundary conditions of crack edge and the concept of finite reciprocal elastic work on the contour enclosing the crack tip.

The SIF solutions of centrally cracked plate with various degree of orthotropy are compared with the boundary collocation solutions. The effect of fiber orientation on the SIF in bidirectional fiber-reinforced composite media is investigated by treating both mode I type of double edge cracked plate in tension and mixed mode type of single edge cracked cantilever plate subjected to end shear.

While the numerical results of the examples above appear to be generally correct, they are far from satisfactory. In particular the results for the mixed mode problem are not numerically independent of choice of the integration contour, although the contour integral is theoretically path independent. This might be a consequence

of the approximate nature of the numerical computation using the data provided by FEM solutions. Furthermore the crude approximation for corner element (4 elements in case of mixed mode) can be possibly associated with the resulting SIF solutions. To obtain more reliable results further study is needed to identify and correct, or at least to minimize the effect of the major error mechanisms. Numerical experiments with different crack geometries, mesh patterns and interpolation forms could be useful.

References

(1) G.C. Sih, P.C. Paris and G.R. Irwin, On Cracks in Rectilinearly Anisotropic Bodies, Int. J. Fracture Mech. 1(3), pp. 189~203, 1965

(2) O.L. Bowie and C.E. Freeze, Central Crack in Plane Orthotropic Rectangular Sheet, Int. J. Fracture Mech. 8(1), pp. 49~58, 1972

(3) S.N. Atluri, A.S. Kobayashi and M. Nakagaki, Application of an Assumed Displacement Hybrid Finite Element Procedure to Two-Dimensional Problems in Fracture Mechanics, AIAA/ASME/SAE 15th Structures, Structural Dynamics and Materials Conference, Las Vegas, Nevada, April 17~19, 1974

(4) S.S. Wang and J.F. Yau, An Analysis of Cracks Emanating from a Circular Hole in Unidirectional Fiber-reinforced Composites, Engng. Fracture Mech. 13, pp. 57~67, 1980

(5) S.S. Wang, J.F. Yau and H.T. Corten, A Mixed-Mode Crack Analysis of Rectilinear Anisotropic Solids using Conservation Laws of Elasticity, Int. J. Fracture, 16(3), pp. 247~259, 1980

(6) J.F. Yau, S.S. Wang and H.T. Corten, A mixed-made Crack Analysis of Isotropic Solids using Conservation Laws of Elasticity, J. Appl. Mech. Trans. ASME, 47, pp. 335~341, 1980

(7) M. Stern, A Boundary Integral Representation of Stress Intensity Factors, Proceedings of 10th Anniversary Meeting of Society of Engineering Science' Raleigh, N.C., Nov. 5~7, pp. 125~132, 1973

(8) M. Stern, E.B. Becker and R.S. Dunham, A Contour Integral Computation of Mixed-mode Stress Intensity Factors, Int. J. Fracture, 12(3), pp. 359~368, 1976

(9) M. Stern and M.L. Soni, On the Computation of Stress Intensities at Fixed-free Corners, Int. J. Solids Struct. 12, pp. 331~337, 1976

(10) Chen-Chin Hong and M. Stern, The Computation of Stress Intensity Factors in Dissimilar Materials, J. Elasticity, 8(1), pp. 21~34, 1978

(11) M.L. Soni and M. Stern, On the Computation of Stress Intensity Factors in Fiber Composite Media using a Contour Integral Method, Int. J. Fracture, 12(3), pp. 331~344, 1976

(12) A.E. Green and W. Zerna, Theoretical Elasticity, Oxford University Press, Oxford, 2nd Ed., 1968

(13) A.H. England, On Stress Singularities in Linear Elasticity, Int. J. Engng. Sci. 9, pp. 571~585, 1971

(14) G.P. Cherepanov, Mechanics of Brittle Fracture. McGraw-Hill, 1979

(15) D. Hull, An Introduction to Composite Materials, Cambridge University Press, 1981

(16) P.C. Paris and G.G. Sih, Stress Analysis of Cracks, Fracture Toughness Testing and Its Application, ASTM STP 381, pp. 30~81, 1965

(17) J.F. Mandell, F.J. McGarry, S.S. Wang and J. Im, Stress Intensity Factors for Anisotropic Fracture Test Specimens of Several Geometries, J. Composite Mat. 8, pp. 106~116, 1974

Appendix

In terms of complex variable $z_k=x-\gamma_k y$, $k=1, 2$ the problems of two-dimensional anisotropic elasticity for equilibrium configurations have solutions with the following representation in terms of the analytic functions $\phi_k(z_k)$ (for example, see ref. (14)) :

$$u_x=2\mathrm{Re}[p_1\phi_1'(z_1)+p_2\phi_2'(z_2)]$$
$$u_y=2\mathrm{Re}[q_1\phi_1'(z_1)+q_2\phi_2'(z_2)]$$
$$\sigma_x=2\mathrm{Re}[\gamma_1^2\phi_1''(z_1)+\gamma_2^2\phi_2''(z_2)] \qquad \text{(A1)}$$

$$\sigma_y=2\mathrm{Re}[\phi_1''(z_1)+\phi_2''(z_2)]$$
$$\tau_{xy}=2\mathrm{Re}[\gamma_1\phi_1''(z_1)+\gamma_2\phi_2''(z_2)]$$

where γ_k, $k=1,2$ are the roots of Eq. (4) and p_k, q_k are the coefficients defined by Eq. (5). Substitution of the following traction free conditions of crack edge,

$$\sigma_y=\tau_{xy}=0\ ;\ x<0,\ y=0$$

into (A1) yields

$$2\mathrm{Re}[\phi_1''(z)+\phi_2''(z)]=0$$
$$2\mathrm{Re}[\gamma_1\phi_1''(z)+\gamma_2\phi_2''(z)]=0 \qquad \text{(A2)}$$

Note that here $z=z_1=z_2$ since we only consider the negative real axis.

The stress intensity factors in terms of ϕ_1 and ϕ_2 can be written as

$$K_{\mathrm{I}}=\lim_{r\to 0}\sqrt{2\pi z}\sigma_y|_{\theta=0}$$
$$=\sqrt{2\pi z}\cdot 2[\phi_1''(z)+\phi_2''(z)]$$
$$K_{\mathrm{II}}=\lim_{r\to 0}\sqrt{2\pi z}\tau_{xy}|_{\theta=0} \qquad \text{(A3)}$$
$$=\sqrt{2\pi z}\cdot 2[\gamma_1\phi_1''(z)+\gamma_2\phi_2''(z)]$$

Now in view of the expressions of Eqs. (A2) and (A3), and the concept of bounded strain energy in an arbitrarily small neighborhood of the crack tip, we may establish the relation between the functions ϕ_1, ϕ_2 and two parameters C_1, C_2 associated with the complementary elastic states

$$C_1=2z^{3/2}[\phi_1''(z)+\phi_2''(z)]$$
$$C_2=2z^{3/2}[\gamma_1\phi_1''(z)+\gamma_2\phi_2''(z)] \qquad \text{(A4)}$$

The order of $z^{3/2}$ can be induced from the fact that the integrand of (2) on the inner boundary appears that a finite contribution will result if $\varepsilon^{1/2}|\underset{\sim}{u}^c|$ and $\varepsilon^{3/2}|\underset{\sim}{T}^c|$ are finite on C_ε.

Inverting Eq. (A4), then we have the following explicit functional forms of ϕ_1, ϕ_2 as

$$\phi_1''(z_1)=\frac{\gamma_2C_1-C_2}{(\gamma_2-\gamma_1)\sqrt{r^3(\cos\theta-\gamma_1\sin\theta)^3}}$$
$$\phi_2''(z_2)=\frac{-\gamma_1C_1+C_2}{(\gamma_2-\gamma_1)\sqrt{r^3(\cos\theta-\gamma_2\sin\theta)^3}} \qquad \text{(A5)}$$

Integration of the above Eq. (A5) produces finally

$$\phi_1'(z_1)=\frac{-\gamma_2C_1+C_2}{(\gamma_2-\gamma_1)\sqrt{r(\cos\theta-\gamma_1\sin\theta)}}$$
$$\phi_2'(z_2)=\frac{\gamma_1C_1-C_2}{(\gamma_2-\gamma_1)\sqrt{r(\cos\theta-\gamma_2\sin\theta)}} \qquad \text{(A6)}$$

and substitution of these functions, ϕ_1 and ϕ_2 into (A1) yields the desired complementary elastic solutions of Eq. (7).